**Benha Journal of Applied Sciences (BJAS)** **print: ISSN 2356–9751**
**Vol. (9) Issue (*) (2024), (57-75)** **online: ISSN 2356–976x**

**http://bjas.bu.edu.eg**

# Numerical Study of Circular Transverse Holes Effect on Reinforced Concrete Circular Columns Under Non-Axial Loads

**A. Montaser[1], A. Abd Elsalam[2], Amr R. Elgamal[2], and Hala. M. Refat[2]**
[1]Corresponding Author, Msc Student, Civil Engineering Department, Benha University, Benha, Egypt
[2]Civil Engineering Department,Benha University, Benha, Egypt
E-mail: eng.montaser2@gmail.com

**Abstract**

For most construction works, engineers have to make holes for various utilities and services with different structural elements. The most critical holes are those in reinforced concrete columns, since the columns are the elements that carry the vertical loads from the floors to the foundation. In the current study, a numerical study of fourteen circular reinforced concrete columns (CRC) with one and two circular transverse holes (CTH) under both axial and non-axial loads is investigated. The circular RC columns have a diameter of 200 mm, a height of 1000 mm, six longitudinal reinforcement steel bars with a diameter of 12 mm, and stirrups with a diameter of 8 mm every 166.6 mm center-to-center spacing. A three-dimensional nonlinear finite element model is conducted using *ABAQUS* Simulia V.6.9 software to investigate the performance of CRC with 63.5 mm diameter CTH that having an area greater than 30% of column diameter under both axial and non-axial loads with different holed locations, 33%, 40%, 50%, and 67% of column height. According to the results, the presence of transverse holes significantly reduces load-carrying capacity, a reduction in ultimate strength ranging from 30% to 41% for columns subjected to axial load, and from 20% to 25%for columns subjected to non-axial load, depending on the number of holes and their location in all specimens. Finally, it was found that the decrease in strength for non-axial loading is much greater than for axial loading, with an average of 30%.

**Keywords:** ABAQUS, CRC, TCH, Non-Linear, Opening

**Abbreviation**

| | |
|---|---|
| $w$ | Displacement of Crack opening |
| $w_c$ | Displacement of Crack opening at which stress can no longer be transferred |
| $c_1$ | Material constant=3 |
| $c_2$ | Material constant=3.93 |
| $G_F$ | Crushing energy or fracture |
| $f_{ck}$ | Cylindrical compressive strength |
| $f_{ctm}$ | Peak concrete tensile strength |
| $E_{cm}$ | Concrete mean elastic modulus |
| $f_{cm}$ | Mean compressive stress |
| $P_{ult}$ | Ultimate load capacity |
| $D$ | Circular Column Diameter |
| $d$ | Circular opening Diameter |
| H | Circular Column Height |
| $n$ | Number of circular openings |
| $e$ | Distance between center of applied load and center of Circular reinforced concrete columns |
| $E$ | Material Modulus of Elasticity |
| $P$ | Material density |
| $u$ | Material Viscosity |
| ***FEA*** | Finite element analysis |
| **CRC** | Circular reinforced concrete column |
| **CTH** | Circular transverse hole |

## 1.Introduction

Reinforced concrete circular columns are the fundamental structural components in various constructions, including buildings and bridges. They are typically designed to carry axial loads, acting directly along their centerline. However, in real-world scenarios, columns may experience non-axial loads due to factors such as wind, eccentrically placed beams, or imperfections during construction.

Circular transverse holes on the behavior of RC circular columns are commonly incorporated for plumbing, electrical conduits, or other service installations. While they serve a functional purpose, their presence can disrupt the structural integrity of the column, particularly under non-axial loading conditions.

Because of such holes, many international structural codes and standards started to consider limits for holes that help owners, developers, and engineers in designing building facilities for withstanding dangerous effect. Despite this crucial use, there hasn't been much study on determining the load-bearing capability of orifice compressive members. Instead, most studies have been mostly empirically based, requiring various researchers to conduct tests in order to assess these aspects. bulk of the study highlights loss in the strength of columns owing to these holes. Among the codes that discussed the issue of holes the **ACI 318 Building Code (2011)** [1] has proposed the limits of the total cross-sectional area occupied by conduits and pipes within a column to 4% for strength calculations.

In the literature there are many available researches that used to investigate the effect of holes in RC Columns.

**Minafo`, 2012[2]** attempted to investigate, using an alternative method of solving the problem, the load carrying capacity of axially loaded RC members with circular openings. Using an experimental analysis and the heretical strut and tie model (STM) for explanation, the author attempted to investigate the columns' ultimate capacity. A hole in an axially loaded member modifies the stress state that already exists. Because of the opening, there will be a geometrical and stress trajectory

discontinuity dispersion; this disturbed region (D region) was examined theoretically using the Struct and Tie Method (STM) **[3]**. The method was applied to determine the bursting tensile force resulting from the rupture of the isostatic lines of stress trajectories, as shown in Figure (1). However, in contrast to bottle-shaped struts, where the tensile fore is positioned in the center of the disturbed D-region, the position of the busting tensile force was close to the hole. According to the findings, placing the hole centers along the column axis had the most detrimental effects. If a sufficient amount of transverse reinforcement was supplied, a significant reduction in load carrying capacity was observed even for a small hole diameter.

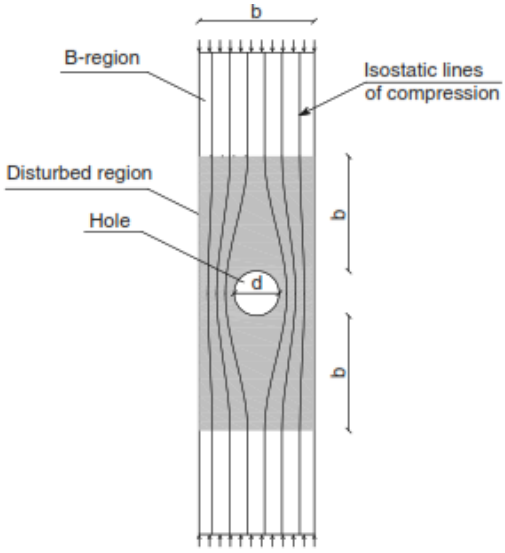


Figure (1) Column with a circular opening: dentition of the disturbed region. (**Redrawn from Minafo`, 2012** [2]

**Ayatullah Khomeni, 2018** [4] investigated the effect of drilled cores on columns' axial capacities using numerical modeling and experimental research. The results of the experiments showed that, depending on the core's location along the column's length, drilling out a core can significantly affect a column's axial capacity. It has been noticed that the capacity reduction of core-drilled columns is largely determined by the strength of the concrete, and that the percentage of capacity reduction of core-drilled columns is somewhat influenced by column tie bar spacing. The concrete exhibited a decrease in capacity of approximately 16% when its compressive strength was reduced to 13.5 MPa. Alternatively, a capacity decrease of approximately 4% was noted for concrete exhibiting a compressive strength of 34.5 MPa. **Tanvir et al., 2015** [5] studied the importance of many aspects impacting the ability of core-drilled columns for safe core extraction, depending on the strength of the concrete and the position of the cores, the extraction of the core has a substantial impact on the axial load bearing capacity of columns. To prevent the stress concentration caused by produced near support and other areas of high stress, it is highly advised to harvest cores from within the middle of columns. Concrete's compressive strength has an impact on how core drilling affects the structural performance of concrete columns. Compared to its counterparts made of high strength concrete, low strength concrete columns shown a considerable drop in axial capacity. This shows that low-strength structures are more susceptible to structural deterioration as a result of core drilling**. Suliman khana, 2019** [6], in light of the information gathered throughout the course of this project's research, have come to the conclusion that "finite element modeling" is the most accurate technique yet created for forecasting the behavior of a structure before it is put into action in a real-world scenario. Also, it is the simplest and most affordable technique to verify the validity of the research by contrasting it with the findings of experiments. Due to different material qualities and environmental conditions, such as temperature, etc., the finite element modeling of the columns predicts a little divergence from the experimental results. **FRAOL NEGASSA, 2020** [7] investigated reinforced concrete with transverse holes numerically. By combining the usage of CFRP wrapping with steel casing, it has been shown that a column with a 100mm hole and one-third of its width may have 99.79 % of its ultimate load capacity restored. The regenerated column's capacity, however, drastically falls if the column cracks past the point of elasticity. A square opening damages 5.69 % more than a circular opening, and providing several holes rather than just one reduces weight bearing ability for a given volume displacement. **Muhammad Fiaz Tahir, 2020** [8] conducted research to determine the impact of a transverse opening in a RC column and to account for the strength lost as a result. It was determined that TCH might cause the specimen's axial strength to decrease by 21%. The most practical solution was determined to be expanding column area to accommodate a TCH. examined RC columns drilled with transverse holes of varying diameters and came to the conclusion that the strength decrease corresponds directly with the strength reduction, which can potentially reach 50%. He is advised to consider the impact of large transverse holes when implementing prescribed slenderness limitations, as holes not only cause strength loss but also contribute to the degradation of stiffness and ductility**.** Under axial stress, the effect of an aperture parallel to the column cross-section's longitudinal axis was examined using both experimental research **(Bakhteri & Iskandar, 2005)** [9] and a numerical simulation **(Al-Maliki et al., 2021)** [10]. In comparison to a column with a solid section, both experiments attested to a notable decrease in axial load capacity brought about by the existence of openings. The axial load capacity that was decreased by longitudinal opening was suggested to be strengthened by increasing longitudinal and transverse reinforcement. By comparing the results obtained from models with and without holes, we aim to quantify the reduction in load capacity and other performance metrics due to the presence of the holes. This knowledge will be crucial for engineers designing RC columns with these features, enabling them to make informed decisions about hole

placement, size, and potential mitigation strategies to ensure structural safety under non-axial loading conditions.

## 2. OBJECTIVES

By employing finite element (FE) analysis using ***ABAQUS*** simulia V.6.9 software, this study aims to comprehensively understand how circular transverse openings influence the performance of RC columns subjected to both of axial and non-axial loads. The FE model will allow for detailed simulations, varying parameters like the number and location of the holes. We will analyze the impact of these variations on critical aspects of the column's behavior, including:

1) Load-carrying capacity: The maximum weight the column can support before failure.
2) Stress distribution: The way internal forces are distributed within the concrete and steel reinforcement.
3) Crack patterns: The development and propagation of cracks under non-axial loading.
4) Deformation behavior: How the column bends or deflects under the applied load.

## 3. RESEARCH METHOD

### 3.1 Model description

The eccentricity ratio and opening position were taken into account as research variables in order to better understand how the circular RC column behaved. Fourteen RC circular column specimens were made based on independent variables in order to examine the behavior of columns with varying opening positions. These columns divided to Two groups A and B every group has Seven columns. The two groups have the same concrete mix and also, are similar in the locations of the 63.5 mm diameter transverse holes, dimensions and contained the same both longitudinal and transverse reinforcement, but *Group "**A**"* are subjected to axial load otherwise the Group ***"B"*** are subjected to eccentric load with eccentricity of 50 mm in the direction parallel to the transversal opening.

The circular RC column measures 1000 mm in height and 200 mm in diameter. SixΦ12 mm steel longitudinal reinforcements and Φ8 mm stirrups with a center-to-center spacing of 166.6 mm were used for the modeling procedure. The details of the tested columns' reinforcement are shown in Figure (2). Column specimens loaded concentrically are shown in Table 1. To put it another way, eccentricity and opening are parallel in Table (2). Measuring from the bottom end of the column, the opening was located at 0.33H, 0.4H, 0.5H, and 0.67H. The primary determinant of position is the significant possibility of stress concentration at the ends and middle of the column as a result of the maximum bending moment and shear force, respectively. The first number in the study specimen designation denotes the group's column number, and the second number indicates the eccentricity's magnitude in millimeters. Each column's details are displayed in Figure (3).

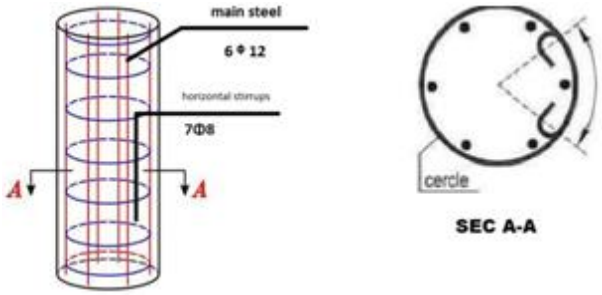


**Figure (2)** Details of reinforcement of tested columns

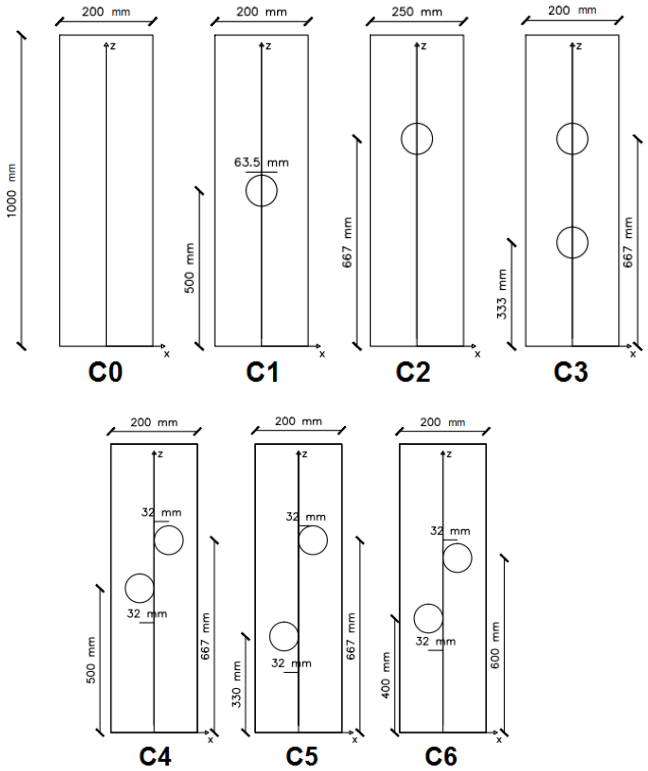


**Figure (3)** Details of holes provided in each column specimen

**Table (1)** Specimens of concentrated-applied reinforced concrete column models

| Direction | Group | Designation | Opening ratio (d/D) | No of holes (n) | Eccentricity ratio (e/D) | Concrete strength (Mpa) | Position of opening (X, Z) | Notes |
|---|---|---|---|---|---|---|---|---|
| Load applied concentrically at center of column | G- A | $C0E_0$ | -------- | ------ - | 0 | 25 | ------- | control |
| | | $C1E_0$ | 0.32 | 1 | 0 | 25 | (0, 500) | |
| | | $C2E_0$ | 0.32 | 1 | 0 | 25 | (0, 667) | |
| | | $C3E_0$ | 0.32 | 2 | 0 | 25 | (0, 330) & (0, 667) | |
| | | $C4E_0$ | 0.32 | 2 | 0 | 25 | (32, 667) & (-32, 500) | |
| | | $C5E_0$ | 0.32 | 2 | 0 | 25 | (-32, 330) & (32, 667) | |
| | | $C6E_0$ | 0.32 | 2 | 0 | 25 | (-32, 400) & (32, 600) | |

**Table (2)** Models specimens where the longitudinal axis of the transverse opening is parallel to the loading eccentricity

| Direction | Group | Designation | Opening ratio (d/D) | No of holes (n) | Eccentricity ratio (e/D) | Concrete strength (Mpa) | Position of opening (X, Z) | Notes |
|---|---|---|---|---|---|---|---|---|
| Load applied concentrically at center of column | G- B | $C0E_{50}$ | -------- | ------- | 0.25 | 25 | ------- | control |
| | | $C1E_{50}$ | 0.32 | 1 | 0.25 | 25 | (0, 500) | |
| | | $C2E_{50}$ | 0.32 | 1 | 0.25 | 25 | (0, 667) | |
| | | $C3E_{50}$ | 0.32 | 2 | 0.25 | 25 | (0, 330) & (0, 667) | |
| | | $C4E_{50}$ | 0.32 | 2 | 0.25 | 25 | (32, 667) & (-32, 500) | |
| | | $C5E_{50}$ | 0.32 | 2 | 0.25 | 25 | (-32, 330) & (32, 667) | |
| | | $C6E_{50}$ | 0.32 | 2 | 0.25 | 25 | (-32, 400) & (32, 600) | |

### 3.2 Material Modeling

#### *3.2.1 Concrete material modeling*

The accuracy of the stress-strain mathematical modeling used to represent the material non-linearity response greatly influences the accuracy of a result obtained from FE simulation. The specimens were modeled using cylindrical compressive strength $f_{ck}$ (MPa)=20 MPa, $E_{cm}$= 28 (MPa) as input, the elastic modulus ($E_{cm}$)is calculated using the formula given in Committee and for Standardization (2002), [11]. Using mathematical formulas and default values for both compressive and tensile stress behavior given in Inc. (2017) [12], concrete damage parameters were calculated.

***A) Concrete compressive behavior***

Identifying an accurate stress relationship for concrete is a challenging task. The uniaxial concrete compressive stress-strain curve and equation given in Committee and for Standardization (2002) [11] were used to obtain concrete compressive stress-strain input data for modeling. For concrete, the uniaxial compressive stress-strain curve is assumed to be linearly elastic up to approximately 30% of the maximum compressive strength. The established non-linear stress-strain response of C-20 concretes under uniaxial compressive loading is displayed in Figure (4-a).

***B) Concrete tensile behavior***

According to Committee & for Standardization, 2002 [11] and M. A. Yusuf Sümer, 2015 [13], the yield stress as a function of displacement or strain can be used to characterize the tensile behavior to taken account for the tension stiffening effect into account. A certain amount of load is transferred to reinforcement and carried by it when concrete cracks. The concrete-damaged plasticity model requires this effect, also referred to as the tension stiffening effect, as an input. The post-failure stress-displacement relationship provides the specification. As can be seen from Equation 1 to Equation 3, the most accurate curve for the extraction of input data for concrete tensile stress-displacement was an exponential function that was proposed in Karihaloo et al., 2003 [14]; H. W., 1986 [14]. To calculate *GF*, Equation 4 was used (Alfarah et al., 2017 [16]). The developed non-linear tensile stress–strain response of *C-20* concretes under uniaxial tensile loading is shown in Figure (4-b). The elastic-plastic characteristics of the concrete used in the FE simulation are shown in Table (3).

$$\frac{\sigma}{f_{ctm}} = f(w) - \frac{w}{w_c} f(w_c) \quad (1)$$

$$(w) = \left[1 + \left(\frac{c_1 w}{w_c}\right)^3\right] e^{\left(-\frac{c_2 w}{w_c}\right)} \quad (2)$$

$$w_c = 5.14 \frac{G_f}{f_{ctm}} \quad (3)$$

$$G_F = 0.073 f_{ctm}^{0.18} \quad (4)$$

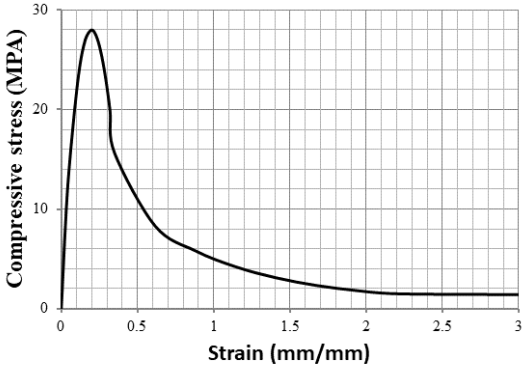


**a**

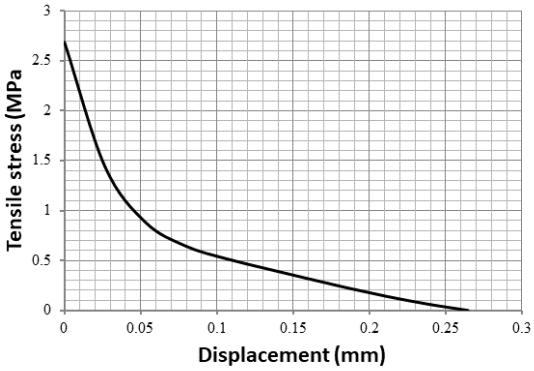


**b**

**Figure (4)** Sample uniaxial stress–strain curve for C-20 **a)** Compression and **b)** tensile

**Table (3)** The elastic–plastic properties of the Concrete

| | | | | |
|---|---|---|---|---|
| **Density** | | | ***P***= 2.4E-09 kg/mm$^3$ | |
| **Elastic** | | | ***E***=28607(MPa), ***u***=0.2 | |
| ***Plasticity*** | | | | |
| **Dilation Angle** | **Eccentricity** | **$F_{bo}/f_{co}$** | **K** | **Viscosity Parameter** |
| 31 | 0.1 | 1.16 | 0.6667 | 0.0001 |

***3.2.2. Steel Material Modeling***

Based on the mathematical modeling suggested in the previous research papers (Hamicha & Kenea, 2022 [17] – Kenea, 2022 [18] – Kenea & Feyissa, 2022 [19] – Maleki & Bagheri, 2008 [120] – Feyissa & Kenea, 2022 [18] – (Megarsa & Kenea, 2022 [21]), ideal bilinear modeling was taken into consideration for this particular study. The steel bar used in the FE simulation has the elastic-plastic characteristics showed in Table (4). The bilinear stress-strain model of the steel curve is shown in Figure (5).

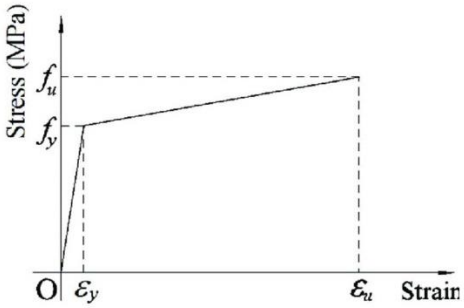


**Figure (5)** the bilinear stress strain model of curve for steel

**Table (4)** The elastic–plastic properties of the Steel Reinforcement

| **Density** | ***P***=7.85E-096 kg/mm$^3$ |
|---|---|
| **Elastic** | ***E***=200E+3(MPa), ***u***=0.3 |
| ***Plastic*** | |
| **Yield Stress (MPa)** | **Plastic Strain** |
| 280 | 0 |
| 360 | 0.1 |

**3.3 Modeling and Simulating**

*ABAQUS* FEA, formerly known as *ABAQUS*, is a package of software applications for computer-aided engineering and finite element analysis that was first launched in 1978. The *ABAQUS* calculator is the inspiration for the name and logo of this program. The *ABAQUS* product suite consists of five essential software applications. For the Finite Element Analysis of Force Displacement Behavior of Reinforced Concrete Column, the *ABAQUS* software was utilized.

**3.3.1 Geometry**

Since the geometry of each component in an *ABAQUS*/CAE model is defined by its parts, these parts serve as the model's building blocks. Native components of *ABAQUS*/CAE can be created.

**3.3.2 Property**

Assigning properties to general contacts in *ABAQUS*/Explicit. Specific areas within the larger contact domain can be governed by the mechanical surface interaction models known as contact properties. These models describe the behavior of surfaces when they intersect.

**3.3.3 Assembly**

Researchers can use an organizational scheme parallel to the physical assembly to generate a finite element mesh using the *ABAQUS* assembly interface. The parts that are assembled together in *ABAQUS* are called part instances. Figure (6) illustrates Model of assembled element.

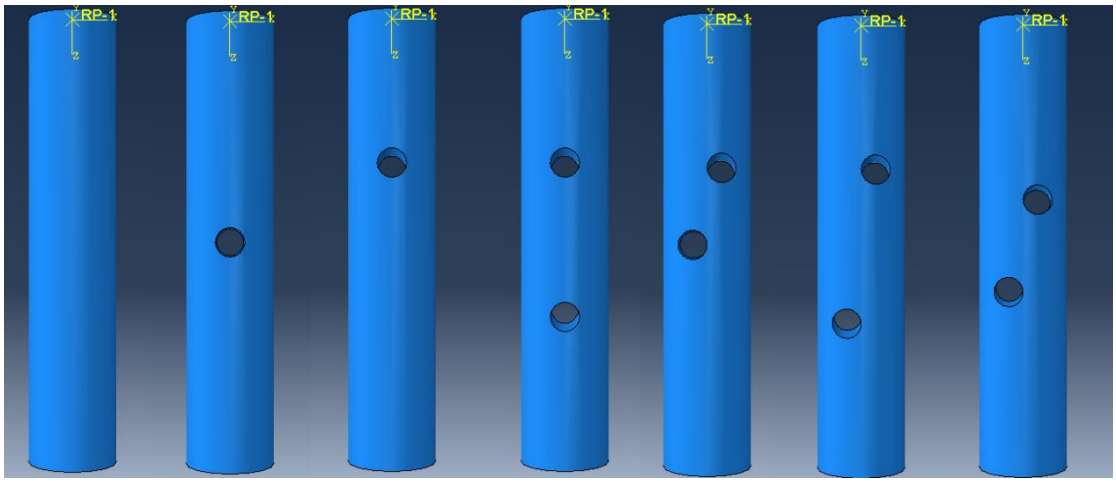


**Figure (6)** Model of element assemble

**3.3.4 Analysis step**

A step can be any convenient period of history, be it thermal, creeping hold, dynamic, etc. In its simplest form, a step in *ABAQUS*/Standard can only be a static analysis of a load change from one magnitude to another. Every step that will be included in the data can have a description provided. Static general is used in the analysis process, where axial displacement of 15 mm is applied to carry out the parametric study of the modeling. In the analysis, the incremental size starts at 0.001 and increases by 1E-028 at a minimum and up to 1 at the maximum. Based on convergence criteria, a maximum of 1000 increments were used during the analysis.

**3.3.5 Interaction**

An all-inclusive surface with all exterior faces, feature edges, analytical rigid surfaces, edges based on beams and trusses, and Eulerian material boundaries are the definition of general contact interactions in *ABAQUS*. By creating a constraint sub-option from the *ABAQUS* interaction module, the interaction between the model's elements is defined. An analytical rigid plate, stirrups, reinforcing steel, and a concrete column are among the parts that were generated. The reinforcement and stirrup element were connected to the concrete column host element using the embedded element option. There is a tie between the analytical rigid plate and the column.

**3.3.6 Boundary condition and load application:**

In a stress/displacement analysis, boundary conditions can be described by the total value of a variable when using the 'direct' format. As many boundary conditions as needed can be defined in a single step. The column's lower end is pinned in every direction. In a stress/displacement analysis, boundary conditions can be described by the total value of a variable when using the 'direct' format. As many boundary conditions as needed can be defined in a single step. The column's lower end is pinned in every direction. A 15 mm vertical displacement in the Z direction can be achieved due to the pins holding the column's top in place in the X and Y directions. The applied load effect was distributed equally over the top end of the column using the analytical rigid plate. The modeling's applied boundary condition and the displacement in the negative Z direction are shown in Figure (7) (A, B) for various scenarios, including those in which there is no opening (solid), openings at 0.33H, 0.4H, 0.5H, and 0.67H, which H was measured from the column bottom end.

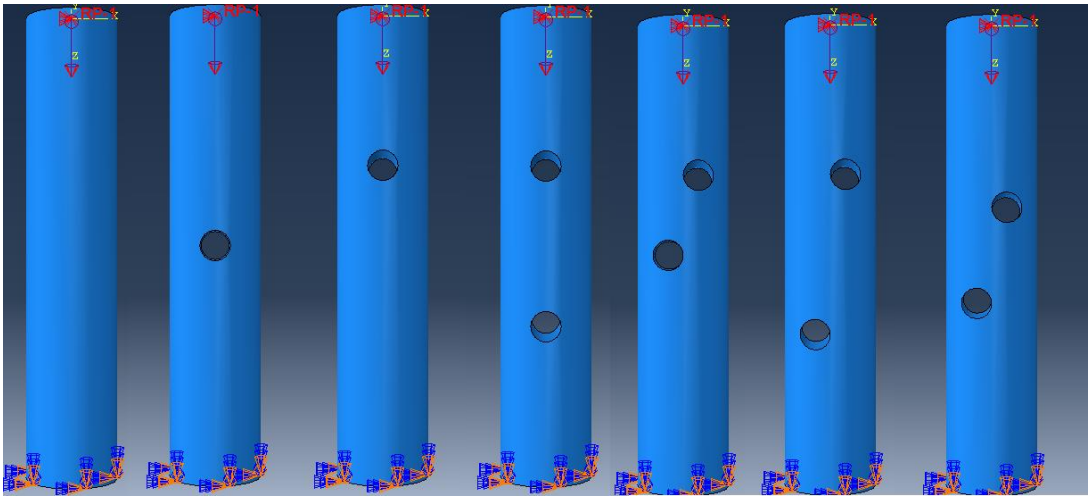

**(a)**

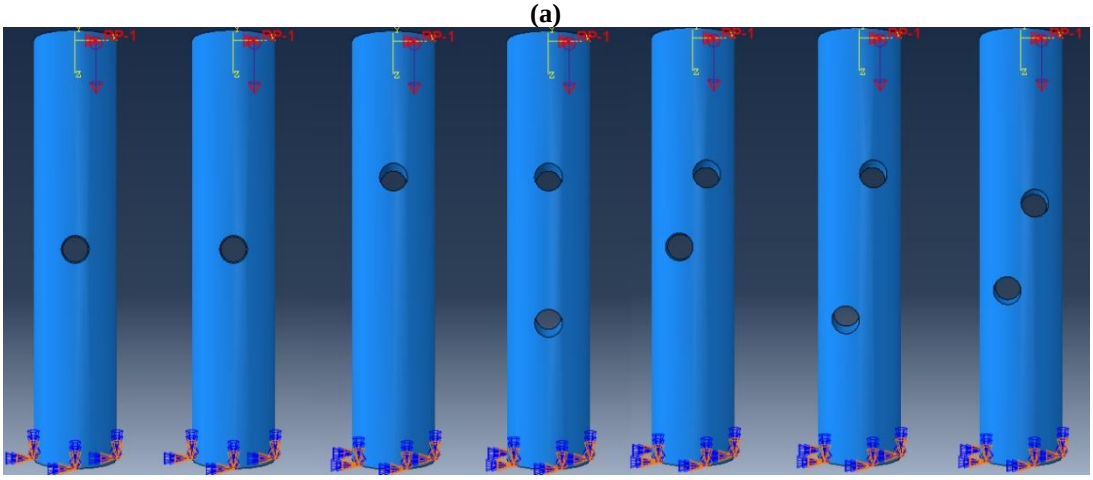

(b)

**Figure (7)** Model of applied load and Boundary condition

**3.3.7 Mesh:**

Using the Finite Element Method, a numerical technique, the main goal of Finite Element Analysis (FEA) is to simulate certain physical phenomena. Based on the model's deformation and force characteristics, the *ABAQUS* model's meshing materials and units better converge during analysis. After conducting many trial runs using different finite element mesh sizes, sufficient accuracy was obtained by the 25 mm mesh size and then selected for this study. With an eight-node reduced integral solid element, the concrete used is C3D8R. Reinforcement uses a two-node truss unit (T3D2). The warp and weft fiber bundles of the fiber woven mesh is taken to be perfect linear elastic materials using a two-node truss unit (T3D2). Figure (8) illustrates the concrete column meshed in the FE simulation with and without open.

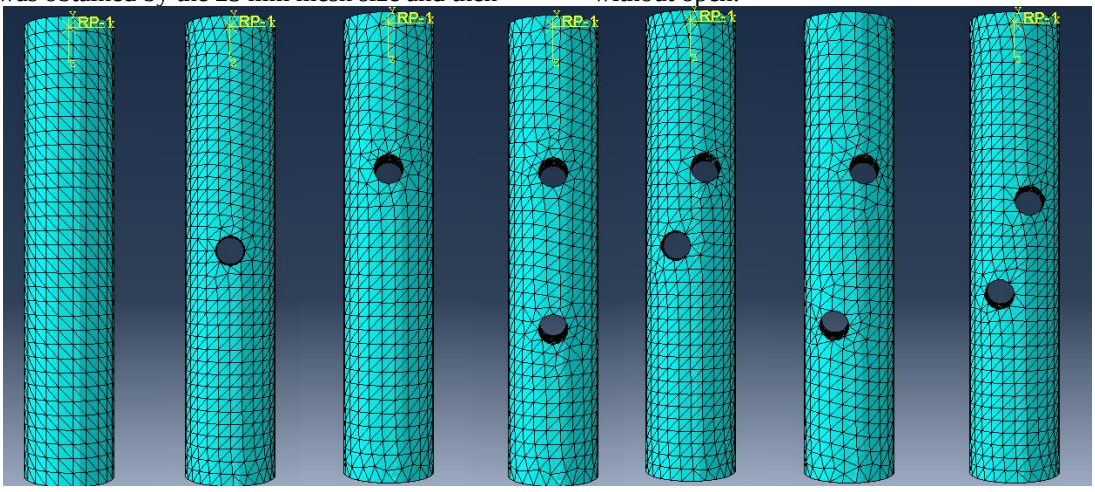

**Figure (8)** RC column mesh in ABAQUS.

## 4.RESULT AND DISCUSSION

### 4.1 Concentrically loaded column

***A) Load – Displacement Curve***

In this category, the opening ratios, number of column holes, and opening positions are taken into account when applying the axial load at the column's center. Figure (9) shows the relationship between the vertical displacement curve and axial load for each loaded column specimen, with the opening position and ratio acting as study parameters. The more column holes or varied opening positions there are, the more the curve's peak point decreases.

***B) Effect of opening number***

Furthermore, the maximum load was likewise lower in all columns with openings than in the control samples, but it was particularly lower in columns with two openings. Table (5) provides the values of the specimens' ultimate strengths derived from the results of the finite element analysis. The ultimate load strength of RC columns is decreased when transverse openings are present. According to the numerical results, there was a 30%–41% decrease in ultimate strength.

***C) Effect of location of opening***

The load-carrying capacity of the RC column is found to be slightly impacted by the position of the openings, according to the analysis. Based on where the holes are located in each specimen in relation to the control column. The ultimate load failure of the columns (C1E0, C2E0, and C3E0) was observed to be 30% lower than that of the control specimen (C0E0). In comparison to the control specimen (C0E0), specimens (C4E0), (C5E0), and (C6E0) likewise attained 40% less strength. This difference might result from taking into account the ideal bond between the reinforcing bars and the concrete also, the numbers position and the distance between the openings. Furthermore, steel bars' linear elastic behavior up until failure may be the cause of this. Therefore, in order to have a safe designed column structure, the effect of the opening's location should be taken into account during the analysis and design of reinforced concrete columns. The combined effects of bending and shear in a frame structure are shown in Table (5).

**Table (5)** Ultimate strengths of concentrically loaded RC column models.

| Direction | Group | Designation | FEA ultimate load *Pult (*KN) | % Difference |
|---|---|---|---|---|
| **Load applied concentrically at center of column** | G- A | $C0E_0$ | 983.4 | ---------- |
| | | $C1E_0$ | 685.9 | 30 % |
| | | $C2E_0$ | 675 | 31% |
| | | $C3E_0$ | 685.6 | 30% |
| | | $C4E_0$ | 557.6 | 43% |
| | | $C5E_0$ | 602.79 | 39% |
| | | $C6E_0$ | 572 | 41% |

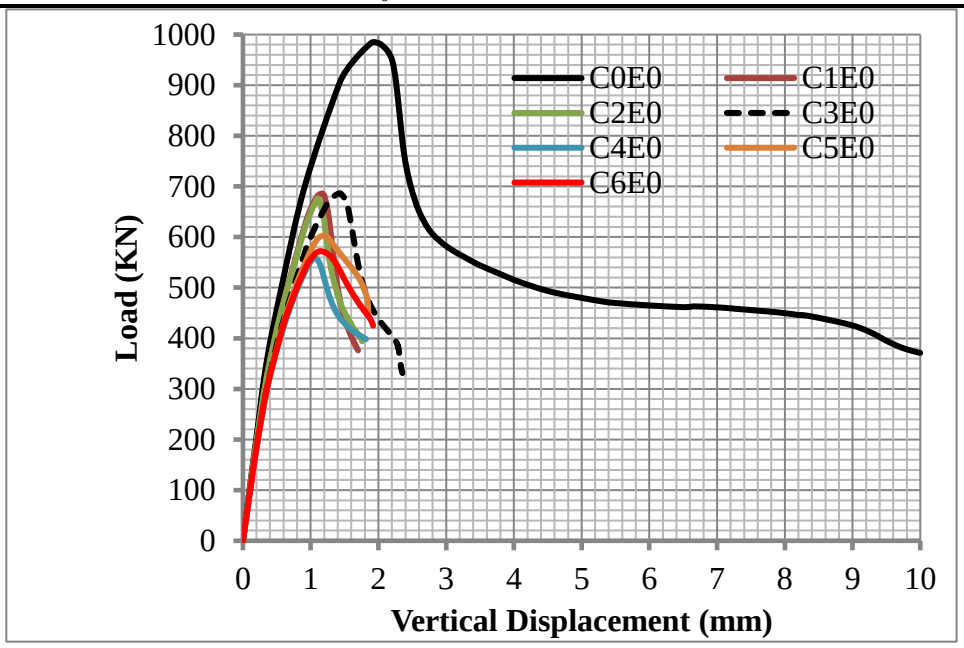


**Figure (9)** Concentrically loaded RC column models' load vs vertical displacement curve.

**4.2 Eccentrically loaded column**

***A) Load – Displacement Curve***

The behavior of the RC column with the transverse opening was also examined by taking into account the load eccentricity effect, which is parallel to the transverse opening's longitudinal axis. A sample of the axial load versus vertical displacement of an eccentrically loaded column is shown in Figure (10), which takes into account the opening ratios, number of column holes, and opening positions.

***B) Effect of opening number***

An opening significantly affects the RC column's axial load capacity. Furthermore, the maximum load was likewise lower in all columns with openings than in the control samples, but it was especially lower in columns with two openings. Table (6) provides the values of the specimens' ultimate strengths derived from the results of the finite element analysis. The ultimate load strength of RC columns is decreased when transverse openings are present. The numerical results indicated a strength reduction of 20% to 25% for columns where the load eccentricity is applied in the direction parallel to the longitudinal axis of opening and tested with eccentricity equal to 50 mm ($e/D$=0.25).

***C) Effect of location of opening***

In this study, the analysis was carried out by making openings at various points along the reinforced concrete column's height. The analysis indicates that the RC column's capacity to withstand a given load is marginally impacted by the location of the openings. Depending on the number of specimens' holes and where they are located. It has been noted that the ultimate load failure of columns C1E0, C2E0, and C3E0 was 20% lower than that of the control specimen C0E0. In addition, specimens C4E0, C5E0, and C6E0 demonstrated 30% lower strength than the control specimen (C0E0). The consideration of a perfect bond between the concrete and reinforcing bars could be the cause of this discrepancy. Furthermore, steel bars' linear elastic behavior up until failure may be the cause of this discrepancy.

**Table (6)** Ultimate strengths of Eccentrically loaded RC column models.

| Direction | Group | Designation | FEA ultimate load *Pult* (KN) | % Difference |
|---|---|---|---|---|
| Load applied concentrically at center of column | G- B | $C0E_{50}$ | 609 | -------- |
| | | $C1E_{50}$ | 478.2 | 20% |
| | | $C2E_{50}$ | 480.2 | 20% |
| | | $C3E_{50}$ | 473.3 | 21% |
| | | $C4E_{50}$ | 411.4 | 31% |
| | | $C5E_{50}$ | 425.9 | 29% |
| | | $C6E_{50}$ | 448.16 | 25% |

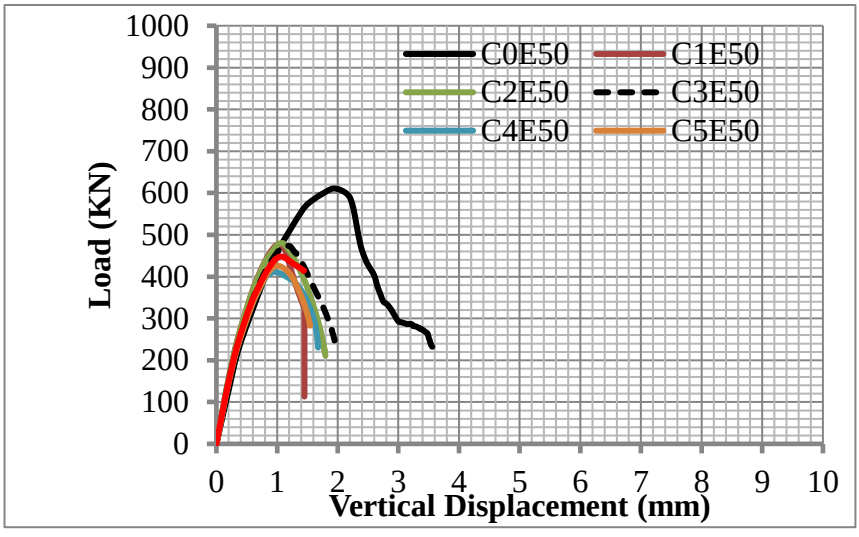


**Figure (10)** Eccentrically loaded RC column models' load vs vertical displacement curve.

### 4.3 Influence of Eccentrically

Comparison of the RC column loaded eccentrically (group B) and concentrically (group A) in terms of ultimate strengths. It has been found that the load non-axial significantly affects both the loaded columns' ultimate strength value and load deflection curve. The findings demonstrated that the ultimate load is significantly reduced as load eccentricity increases. When axial loading and non-axial loading are compared, it becomes apparent that the strength decreases by an average of 30% more with non-axial loading than with axial loading. This indicates that the strength decreases significantly with non-axial loading, depending on the number and location of holes in all specimens. Figure (11) illustrates the Difference between the ultimate strengths of RC column models loaded eccentrically (group A) and concentrically (group B).

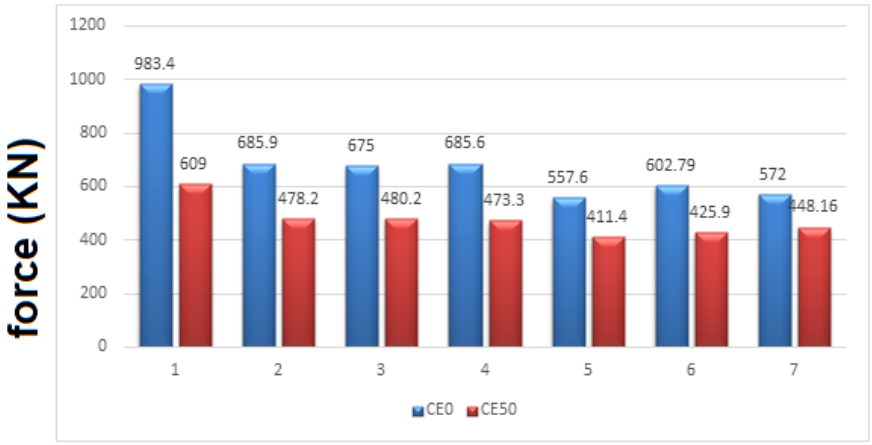


**Figure (11)** The difference between the ultimate strengths of RC column models loaded eccentrically (group A) and concentrically (group B).

### 4.4 Damaging mode

Based on the concentration of stress, the most damaged region of the model specimens can be identified using damage or failure mode. A certain number of specimens were examined by taking into account the various opening positions and eccentricity ratios for both compressive and tensile damage because the damage mode of all the specimens was nearly identical. The geometric condition of the specimens and the type of loading can both contribute to non-uniformity in stress concentration. Figures (12) through (25) show the compressive damage versus strain and the compression damage mode. Tensile damage mode and tension damage versus displacement are shown in Figures (26–39). The results of the study showed that the geometric discontinuity around the opening causes a high-stress concentration. As a result, the model's surrounding elements are more impacted than other areas. Around the transverse opening, compression and tension caused damage to a significant section of the RC column. Damage from tension and compression is more severe in the column's highlighted region. The contour visualization shows that the concentrated compression and tension stresses cause damage to the sections of the reinforced concrete column surrounding openings. Compression and tension cause damage to large sections of concrete columns.

**Figure (12)a)** Compressive damage and **b)** Compressive damage vs strain curve for C0E0

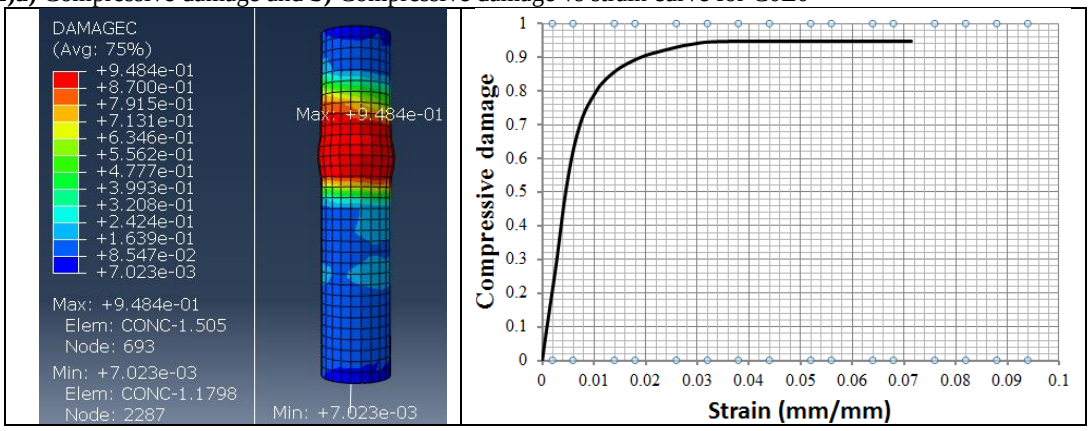


**Figure (13) a)** Compressive damage and **b)** Compressive damage vs strain curve for C1E0

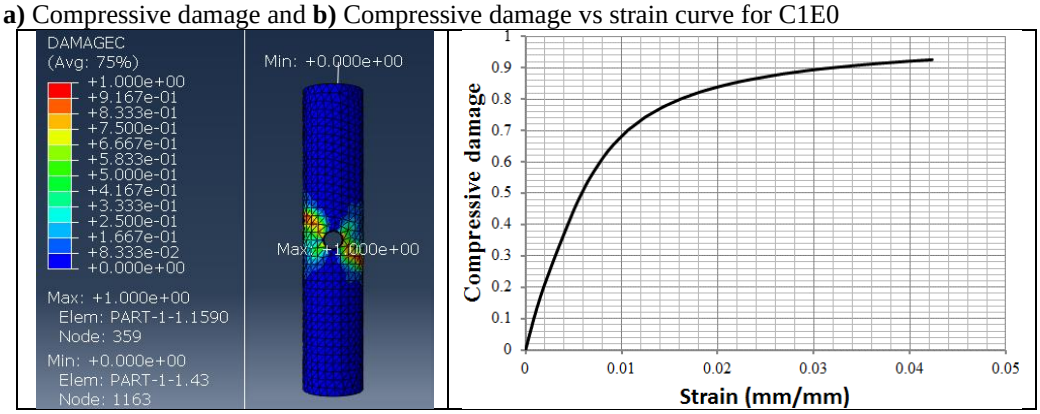


**Figure (14) a)** Compressive damage and **b)** Compressive damage vs strain curve for C2E0

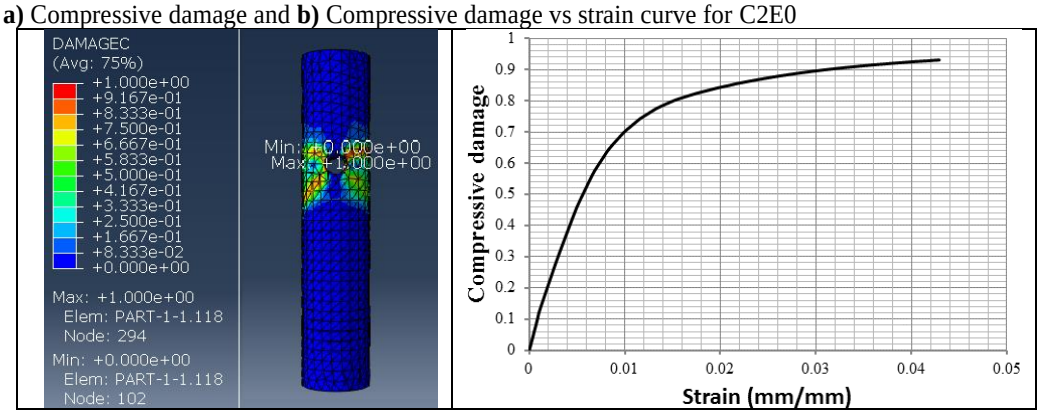


**Figure (15) a)** Compressive damage and **b)** Compressive damage vs strain curve for C3E0

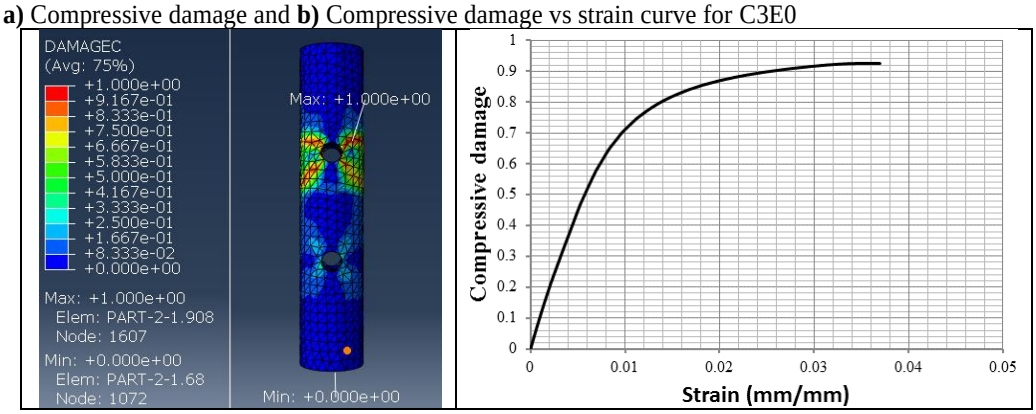

**Figure (16) a)** Compressive damage and **b)** Compressive damage vs strain curve for C4E0

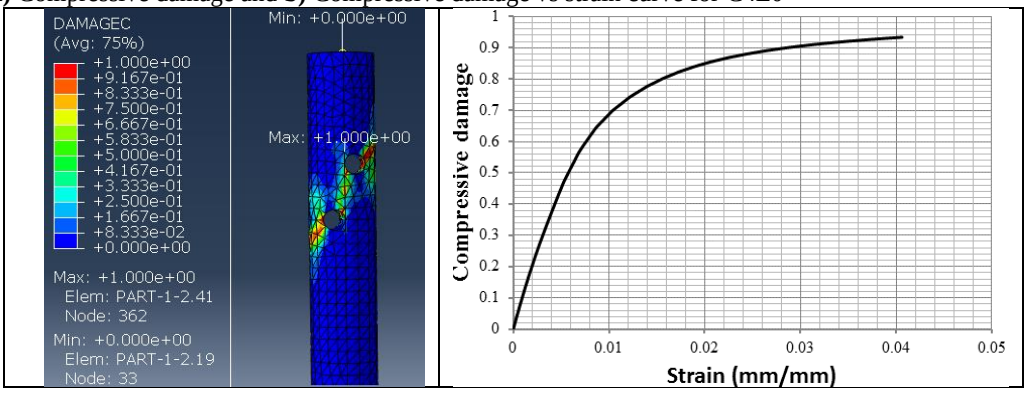


**Figure (17) a)** Compressive damage and **b)** Compressive damage vs strain curve for C5E0

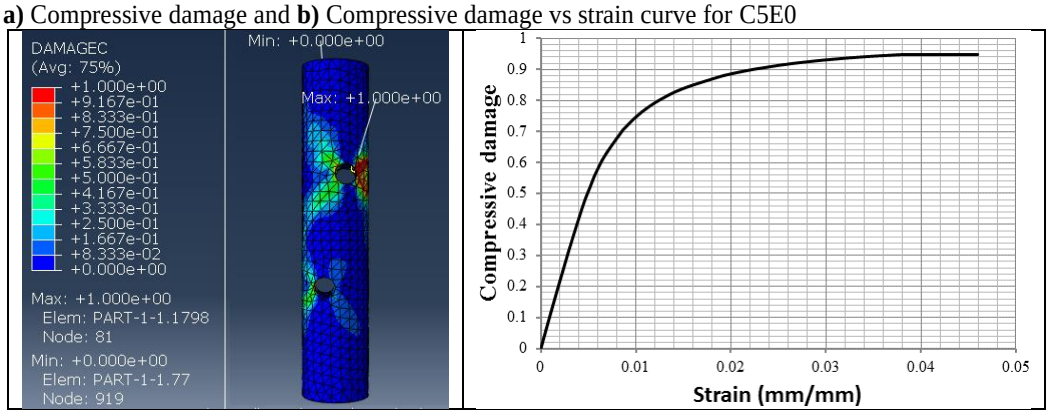


**Figure (18) a)** Compressive damage and **b)** Compressive damage vs strain curve for C6E0

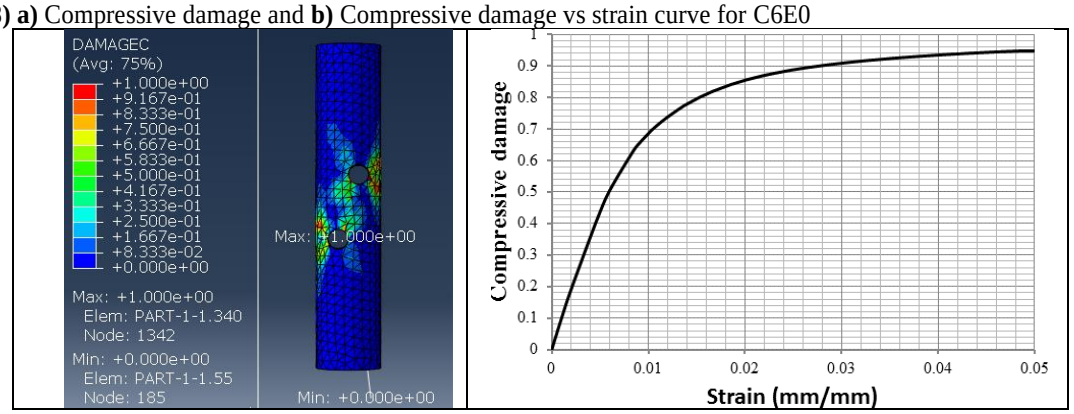


**Figure (19) a)** Compressive damage and **b)** Compressive damage vs strain curve for C0E50

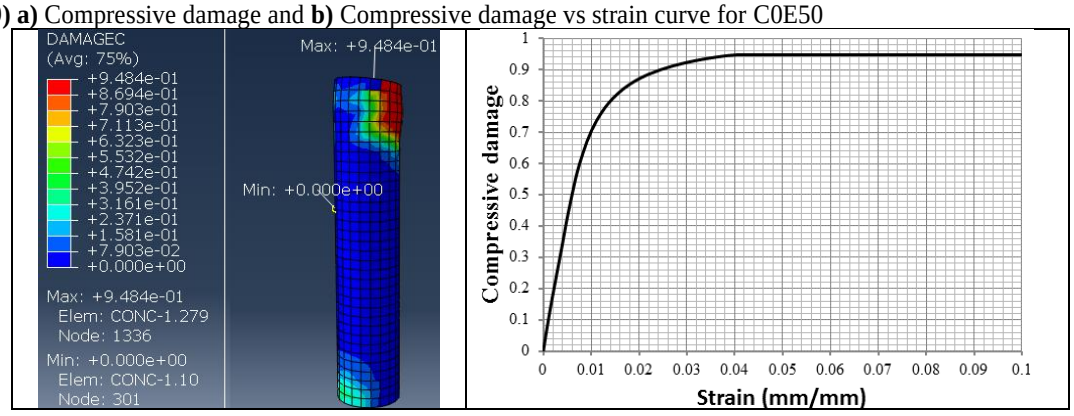

**Figure (20) a)** Compressive damage and **b)** Compressive damage vs strain curve for C1E50

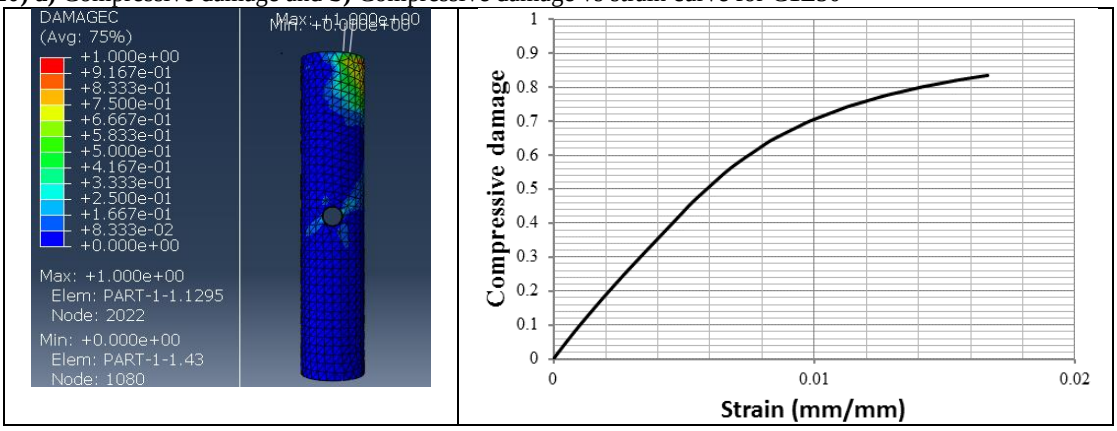


**Figure (21) a)** Compressive damage and **b)** Compressive damage vs strain curve for C2E50

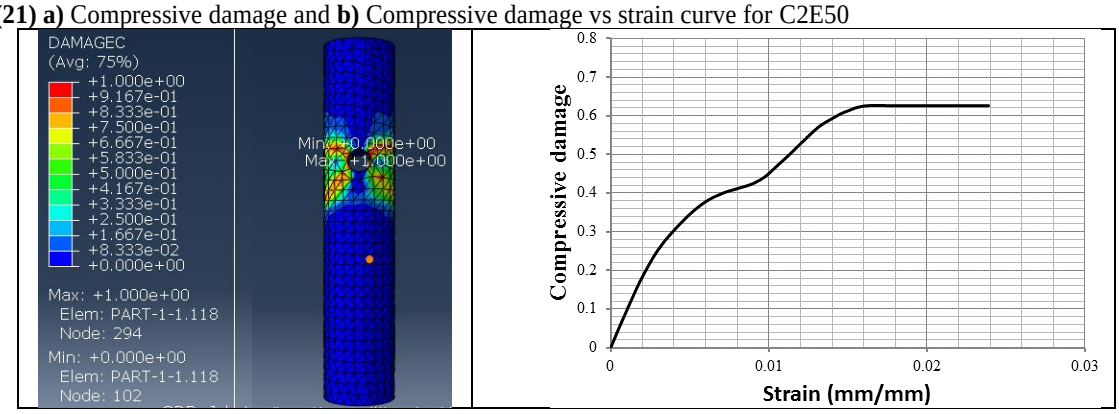


**Figure (22) a)** Compressive damage and **b)** Compressive damage vs strain curve for C3E50

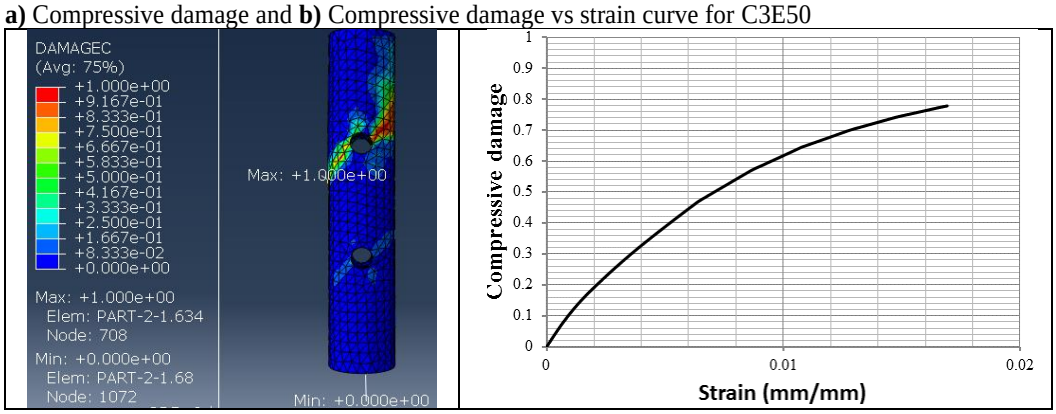


**Figure (23) a)** Compressive damage and **b)** Compressive damage vs strain curve for C4E50

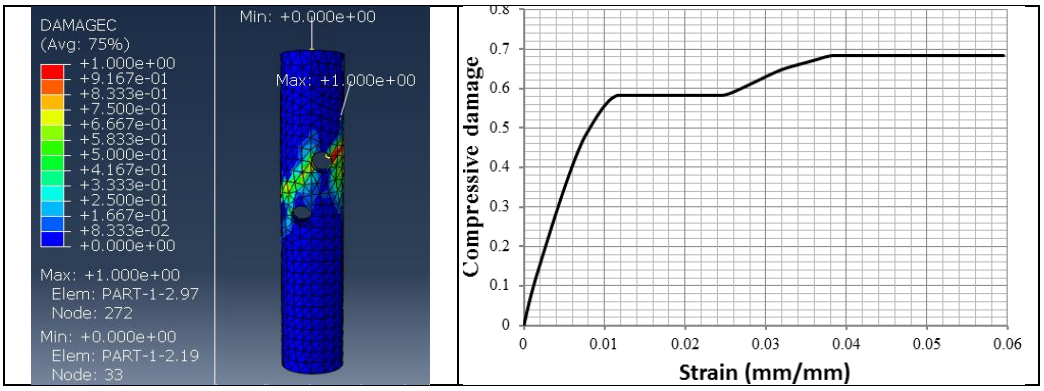

**Figure (24) a)** Compressive damage and **b)** Compressive damage vs strain curve for C5E50

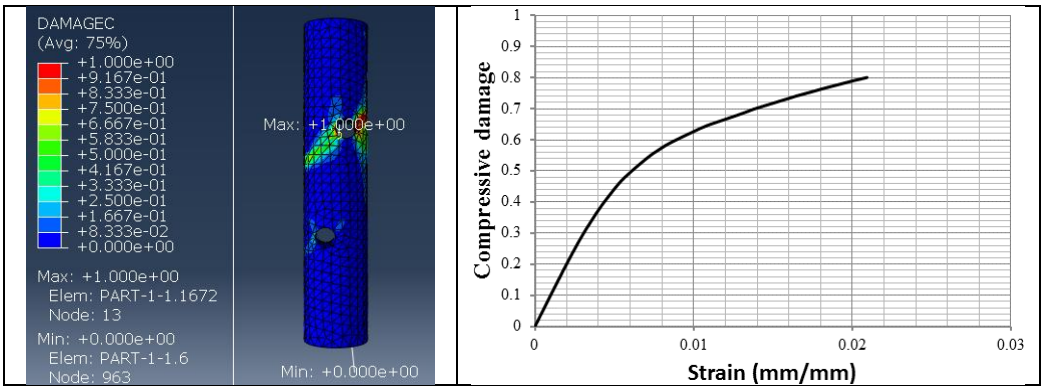


**Figure (25) a)** Compressive damage and **b)** Compressive damage vs strain curve forC6E50

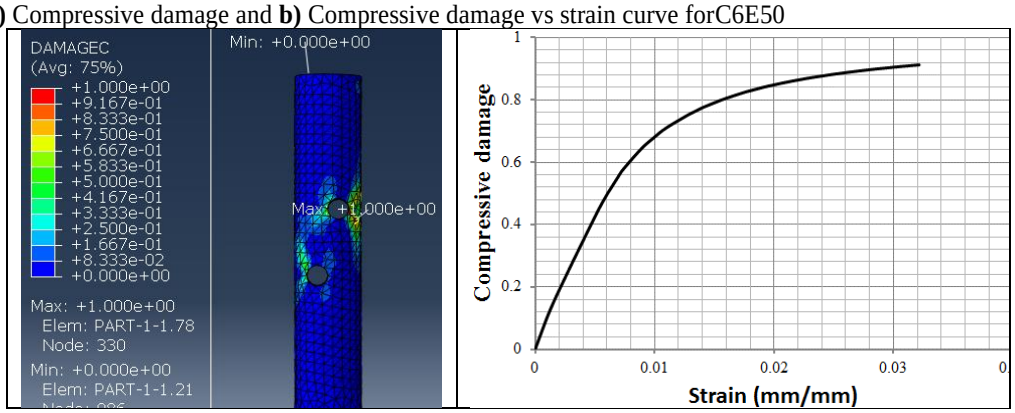


**Figure (26) a)** Tensile damage and **b)** Tensile damage vs displacement curve for C0E0

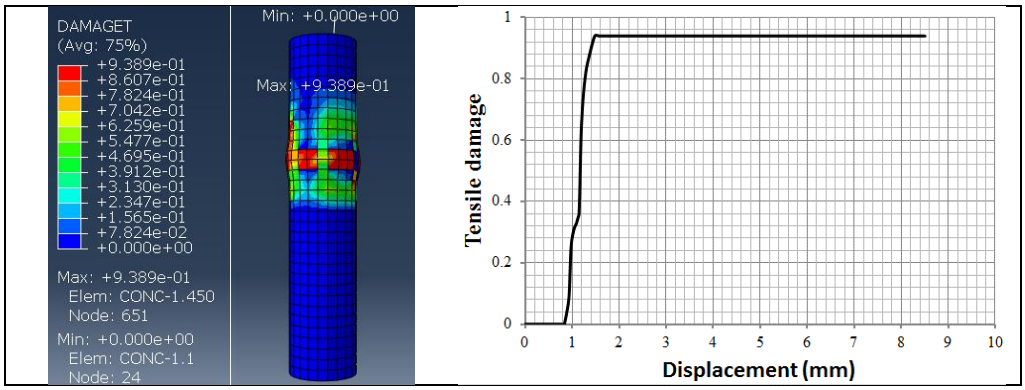


**Figure (27) a)** Tensile damage and **b)** Tensile damage vs displacement curve for C1E0

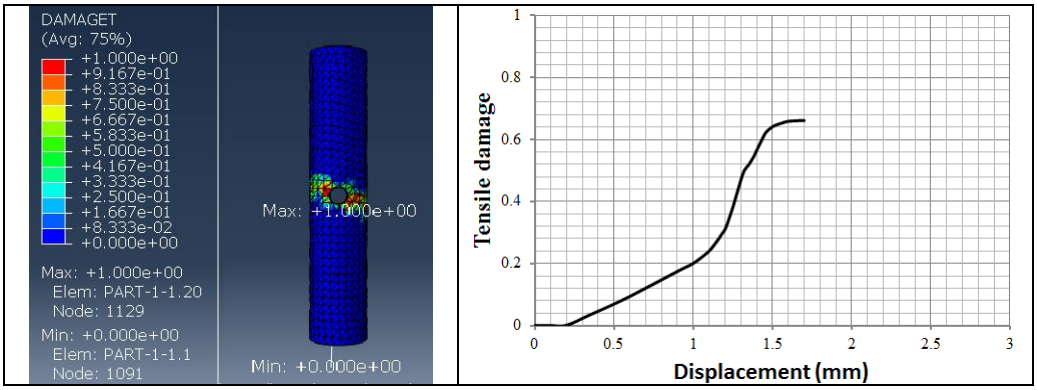

**Figure (28) a)** Tensile damage and **b)** Tensile damage vs displacement curve for C2E0

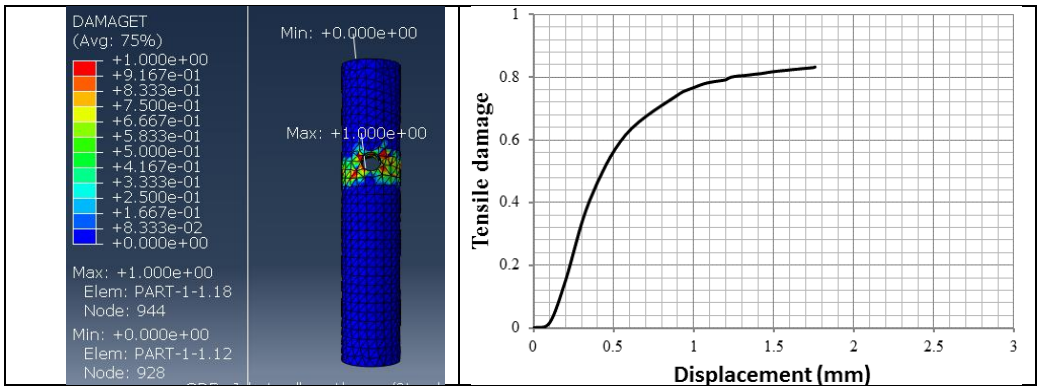


**Figure (29) a)** Tensile damage and **b)** Tensile damage vs displacement curve for C3E0

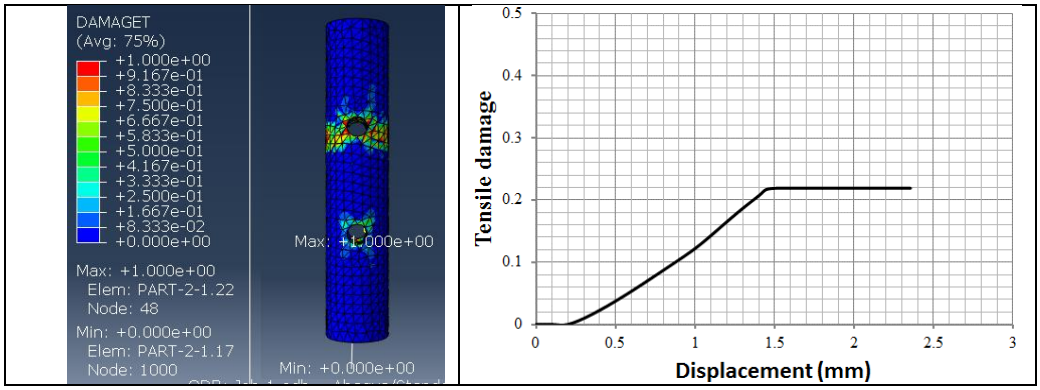


**Figure (30) a)** Tensile damage and b**)** Tensile damage vs displacement curve for C4E0

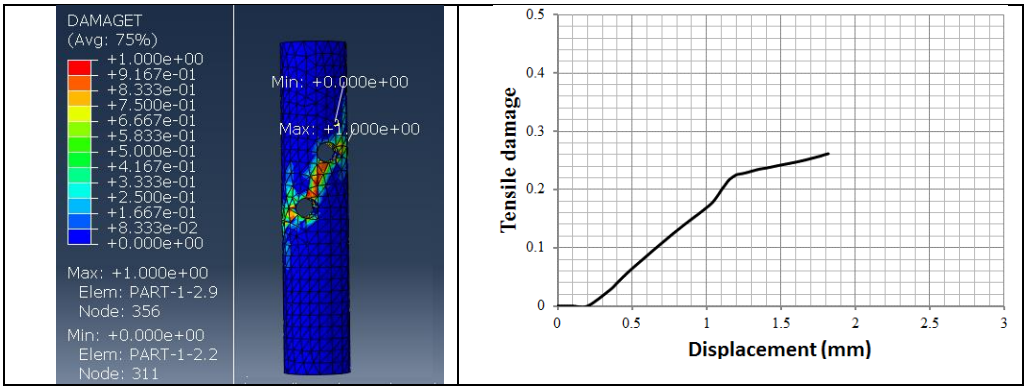


**Figure (31) a)** Tensile damage and **b)** Tensile damage vs displacement curve for C5E0

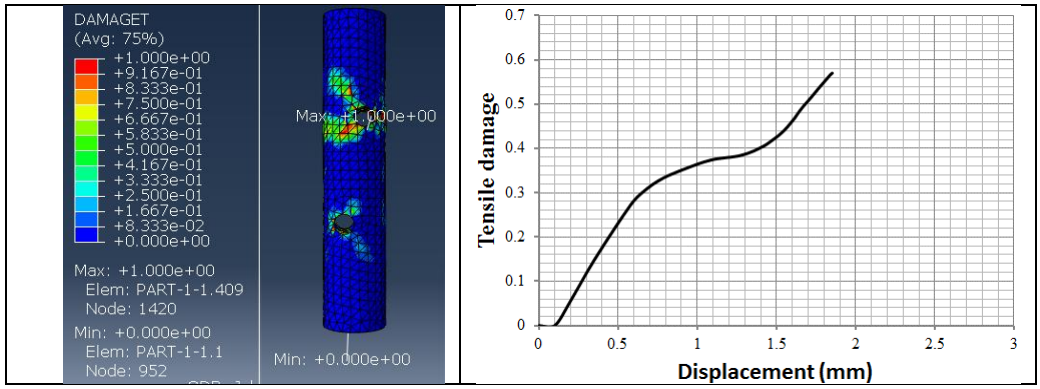

**Figure (32) a)** Tensile damage and **b)** Tensile damage vs displacement curve for C6E0

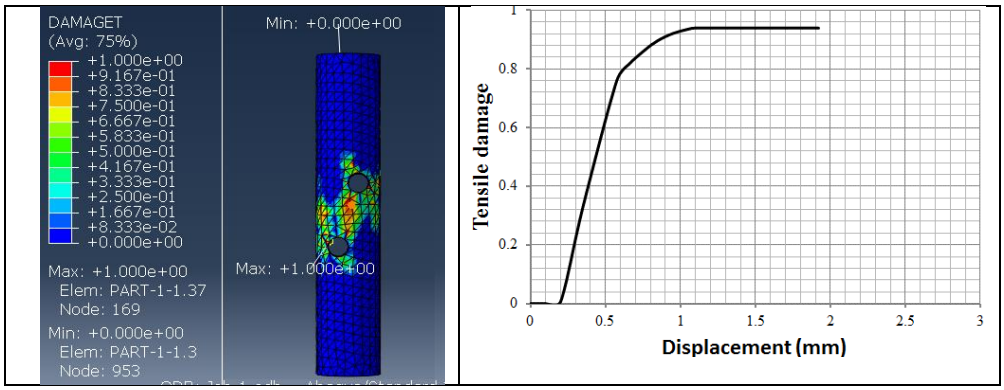


**Figure (33) a)** Tensile damage and **b)** Tensile damage vs displacement curve for C0E50

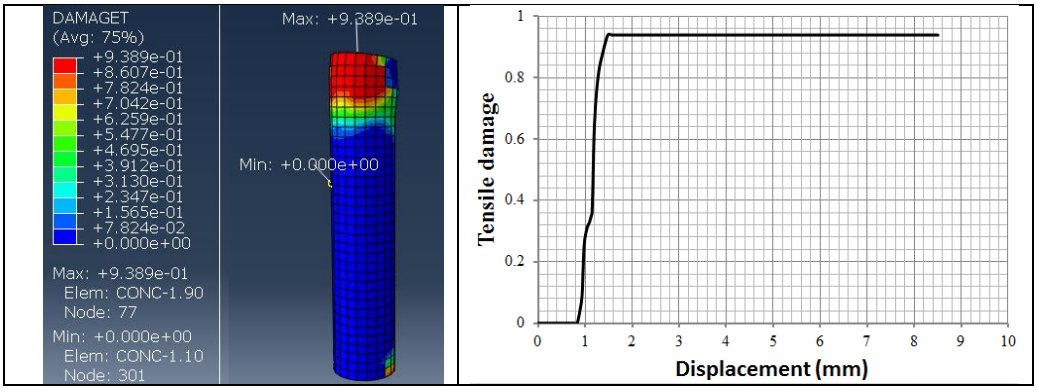


**Figure (34) a)** Tensile damage and **b)** Tensile damage vs displacement curve for C1E50

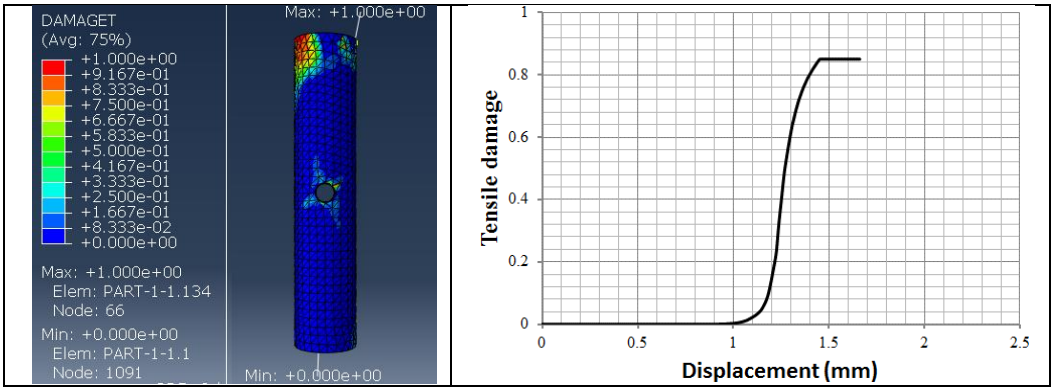


**Figure (35) a)** Tensile damage and **b)** Tensile damage vs displacement curve for C2E50

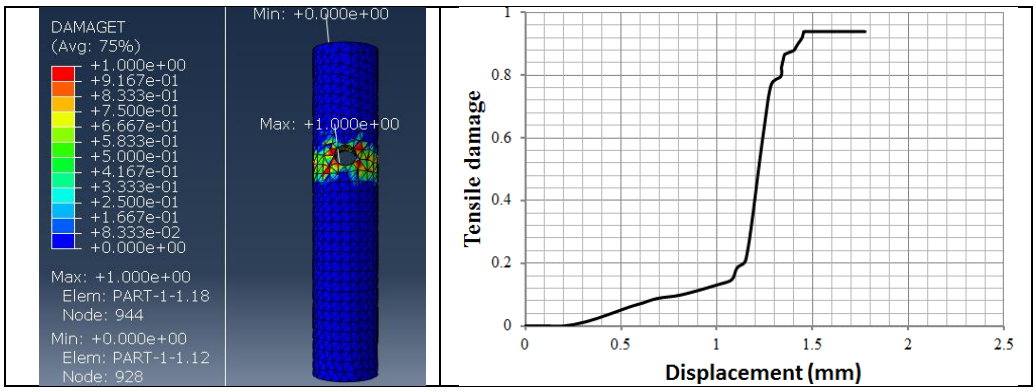

**Figure (36) a)** Tensile damage and **b)** Tensile damage vs displacement curve for C3E50

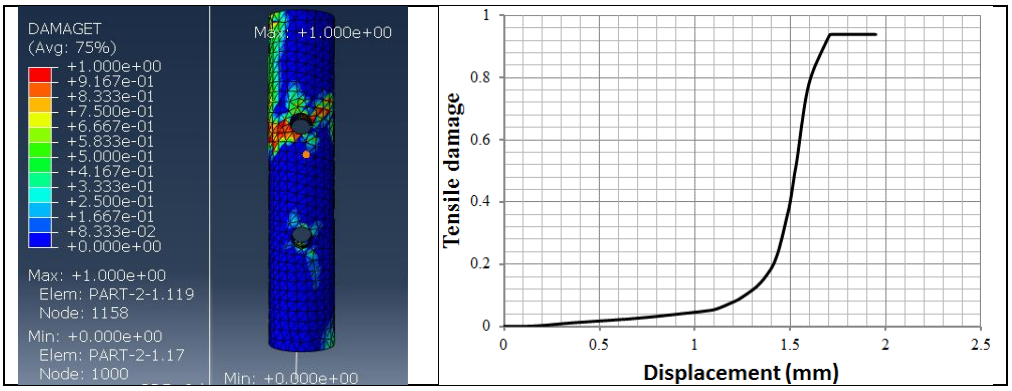


**Figure (37) a)** Tensile damage and **b)** Tensile damage vs displacement curve for C4E50

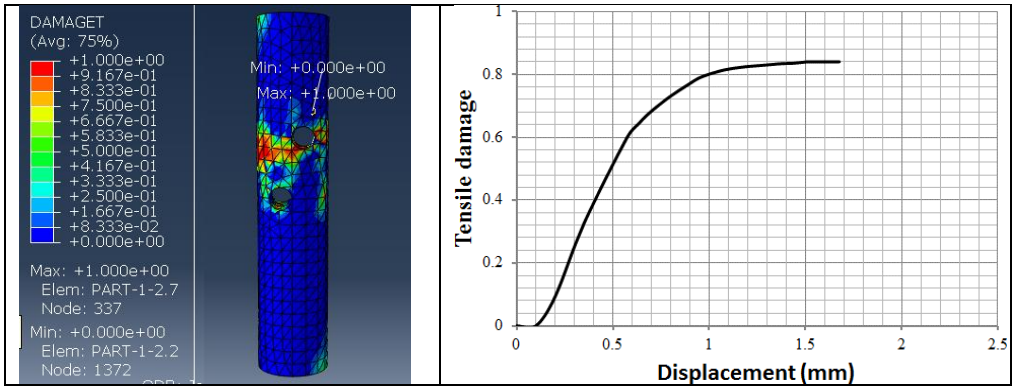


**Figure (38) a)** Tensile damage and **b)** Tensile damage vs displacement curve for C5E50

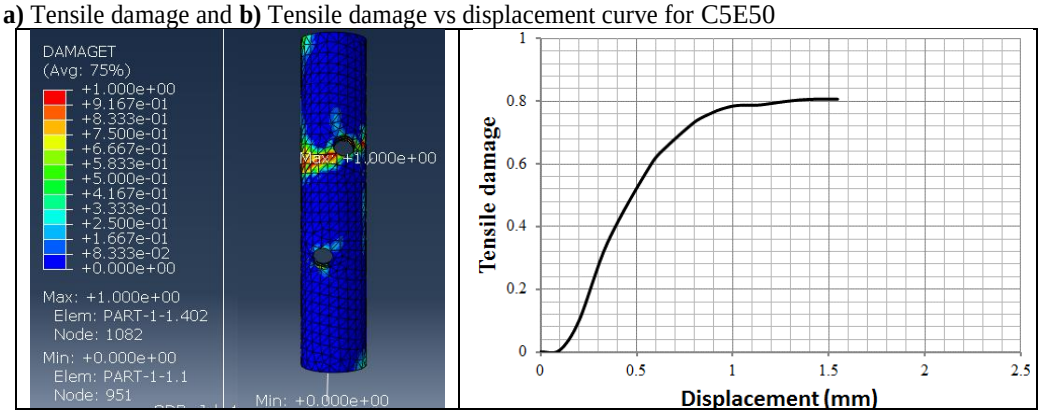


**Figure (39) a)** Tensile damage and **b)** Tensile damage vs displacement curve for C6E50

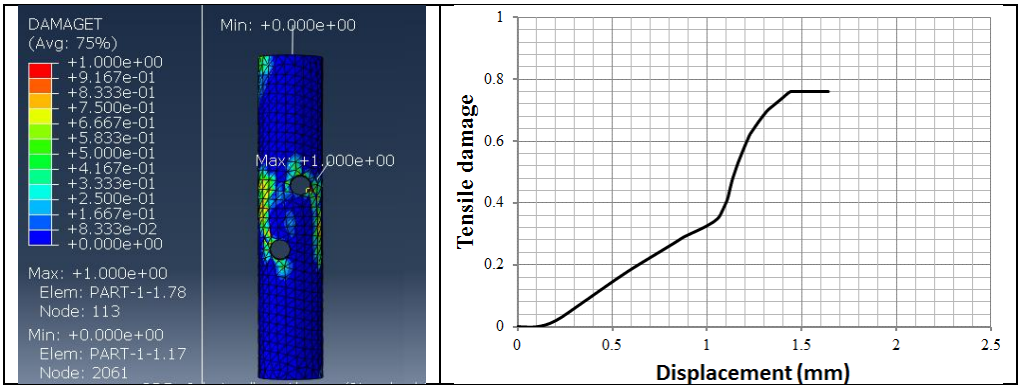

## 5. CONCLUSION

To find out how the number, location, and eccentricity of the openings parallel to the longitudinal axis of the transverse opening affect the ultimate load capacity of the circular reinforced concrete columns with one or two circular transverse holes, an intensified non-linear FE analysis has been modeled in *ABAQUS* software. Additionally, based on the outcome of the FE simulation, the damage mode (tensile and compression damage) of the RC column in the presence of an opening has been examined. The following conclusion has been made based on the outcome of the FE simulation:

1. The ultimate load strength of CRC columns is decreased when transverse openings are present. The ultimate strength of columns under pure compressive axial load was found to be reduced by 30% to 41%, according to the results. Depending on the total number of specimens' holes and where they are located.
2. Depending on the number of holes and where they are located throughout all specimens, the analytical Simulation results for columns with load eccentricity applied in the direction parallel to the longitudinal axis of opening and examined with eccentricity equal to 50 mm ($e/D$=0.25) showed a decrease in strength that varied from 20% to 25%.
3. It has been found that the non-axial load significantly affects both the CRC columns' ultimate strength value and load deflection curve. The findings demonstrated that the ultimate load is significantly reduced as load eccentricity increases. When axial loading and non-axial loading are compared, it is found that the strength decreases by an average of 30% more with non-axial loading than with axial loading. This indicates that the strength decreases significantly with non-axial loading, depending on the number and location of holes in all specimens.

## 6. RECOMMENDATION

The scope of this study was focused on examining the effects of eccentricity parallel to the longitudinal axis of the transverse opening, number of openings, and position of openings on the ultimate load capacity of circular reinforced concrete columns with one or two circular transverse holes. It is suggested that research be conducted on circular column behavior in to identify: -

1. Effect of opening ratio,
2. The influence of concrete density,
3. Effects of eccentricity ratio perpendicular to and normal to the opening axis,
4. Lateral loads' affect.

## ACKNOWLEDGEMENTS

Special thanks to the Civil Engineering Department of the ***Benha Faculty of engineering.***

## FUNDING

For this specific study, there is no funding source.

## DATA AVAILABILITY STATEMENT

The manuscript has all the necessary data.

## DECLARATIONS AND COMPLIANCE WITH ETHICAL STANDARDS

**Conflict of interest** Regarding the paper, the authors declare that they have no conflicts of interest.

## References

[1] Farmington Hills, American Concrete Institute (ACI) Committee 318. (2011). Building Code Requirements for Structural Concrete (ACI 318-11) ISBN 978-0-87031-744-6

[2] Minafo, G. (2012). Load-carrying capacity of axially-loaded RC members with circular openings. Engineering Structures, 41(1), 136–145. DOI: 10.1016/j.engstruct.2012.03.042

[3] Khater, M. (2016). Analysis of Reinforced Concrete D-Regions Using Strut-and-Tie Model. The Egyptian International Journal of Engineering Sciences and Technology, 20(1), 25-37. DOI: 10.21608/eijest.2016.97173

[4] Ayatullah Khomeni, (2018) Experimental investigation and numerical simulation on effect of drilled cores on axial capacity of columns, *Bangladesh University Engineering* and *Technology*, Eng Struct 1014042322F

[5] N. H, Al-Salim, 2021. Behavior and Stress Analysis around Openings for Reinforced Concrete Columns, International Journal of Chemical, Environmental & Biological Sciences (IJCEBS) Vol. 3, Issue 5, ISSN 2320–4087 (Online), pp. 404 – 407.

[6] Suliman khana, and Muneer Ahmed. (2019) Experimental Study and Finite Element Modelling of Reinforced Concrete Column Having an Opening. University of Engineering and Technology Taxila, Pakistan. ISSN 2225-0581

[7] Fraol Negassa. (2020). Numerical Investigation of Reinforced Concrete Columns With Transverse Holes. Issn 2320-9186. https://doi.org/10.20372/NADRE/6413

[8] Tahir, M. F., Shabbir, F., Ahmad, A., & Ejaz, N. (2020). Experimental and numerical investigation of transverse circular holes on load-carrying capacity of RC columns. Iranian Journal of Science and Technology: Transactions of Civil Engineering, 45(1), 1-13. DOI: 10.1007/s40996-020-00372-2

[9] Bakhteri, J., Iskandar, S. A. (2005). Experimental study of reinforced concrete columns concealing rainwater pipes. Jurnal Teknologi, 43(1), 13–26.

[10] Al-Maliki, H. N. G., Alshimmeri, A. J. H., Ali, A. M., Madhloom, H.M., & Gamil, Y. (2021). Nonlinear simulation analysis of tapered reinforced concrete column (solid and hollow) behavior under axial load. Geomate Journal, 21(86), 131–146.

[11] European Committee for Standardization (2004). Eurocode 2: Design of concrete structures - Part 1-1: General rules and rules for buildings. EN 1992-1-1:2004 (E).

[12] Dassault Systèmes Simulia Corp. (2017). ABAQUS Version 6.10–1 Analysis User's Manual. [Online]. Available: 130.149.89.49:2080/v6.10/pdf_books/ANALYSIS_3.pdf

[13] Yusuf Sumer, M. A. (2015). Defining parameters for concrete damage plasticity model. *Challenge Journal of Structural Mechanics*.doi.org/10.20528/cjsmec.2015.07.023

[14] Karihaloo, B. L., Abdalla, H. M., & Imjai, T. (2003). A simple method for determining the true specific fracture energy of concrete. Magazine of Concrete Research, 55(5), 471–481. DOI: 10.1680/macr.55.5.471.37590

[15] Hordijk, D. A., & Reinhardt, H. W. (1986). Experimental determination of crack softening characteristics of normal weight and lightweight concrete. Materials Science, 31(2), 45.

[16] Alfarah, B., Lopez-almansa, F., & Oller, S. (2017). New methodology for calculating damage variables evolution in Plastic Damage Model for RC structures. *Engineering Structures*, *132*, 70–86. DOI: 10.1016/j.engstruct.2016.11.022

[17] Hamicha, A., & Kenea, G. (2022). "Investigation on the effect of geometric parameter on reinforced concrete exterior shear wall slab connection using finite element analysis." Advances in Civil Engineering,1,17. DOI: 10.1155/2022/4903650

[18] Kenea, G. (2022). Analytical study of geometric parameter effect on the behavior of horizontally curved reinforced concrete deep beam. Journal of Engineering, 2022, 1–14. DOI: 10.1155/2022/8052852

[19] Kenea, G., &Feyissa, A. (2022). Cyclic behavior of reinforced concrete slab-column connection using numerical simulation. Advances in Civil Engineering, 2022, 1–14. DOI: 10.1155/2022/2814715

[20] Maleki, S., & Bagheri, S. (2008). Behavior of channel shear connector Part II: Analytical study. Journal of Constructional Steel Research, 64(12), 1341–1348 DOI: 10.1016/j.jcsr.2008.01.010

[21] Megarsa, E., & Kenea, G. (2022). "Numerical investigation on shear performance of reinforced concrete beam by using ferrocement composite." Mathematical Problems in Engineering., 1, 12. DOI: 10.1155/2022/5984177